Journal of Alloys and Compounds 593 (2014) 123–127

Contents lists available at ScienceDirect

Journal of Alloys and Compounds

journal homepage: www.elsevier.com/locate/jalcom

Dependence of optical and thermal properties on concentration and temperature for Yb:YAG laser ceramics

Fei Tang [a,b], Wenchao Wang [a], Xuanyi Yuan [a], Chen Zhu [a], Jiquan Huang [b], Chaoyang Ma [a], Fangyu Wang [a], Yue Lin [b], Yongge Cao [a,b,*]

[a] Department of Physics, Renmin University of China, Beijing 100872, China
[b] Key Lab of Optoelectronic Materials Chemistry and Physics, Fujian Institute of Research on the Structure of Matter, Chinese Academy of Sciences, Fuzhou 350002, China

ARTICLE INFO

Article history:
Received 14 October 2013
Received in revised form 20 December 2013
Accepted 21 December 2013
Available online 3 January 2014

Keywords:
YAG laser ceramics
Absorption edge
Fluorescence property
Thermal diffusivity
Laser performance

ABSTRACT

This paper reports the influence of temperature and doping concentration on optical and thermal properties of Yb:YAG transparent ceramics. The rise of Yb doping concentration causes the gradual red-shift of absorption edge, and both Yb^{3+}absorption coefficient and fluorescence lifetime increases. For 5% Yb:YAG ceramic, as temperature increases from 100 K to room temperature, the fluorescence intensity decreases with broadening of each peak. By using a 940 nm diode laser as the pumping source, we obtained a high slope efficiency of 49% for 5%Yb:YAG ceramics, compared with 41% for 10%Yb:YAG ceramic.

1. Introduction

Since the first demonstration of Nd:YAG ceramic laser in 1995 [1], the past two decades have witnessed the whole development of YAG ceramic laser materials [2–11]. Recently, some researchers have shown strong interest on other ceramics like CaF_2, LuAG and Lu_2O_3 [12–15]. However, these materials do not shows obvious advantages compared to YAG ceramics. As one of potential candidates for high-power laser materials, Yb:YAG ceramics have always gained much attention because of the superior physical properties of Yb ions, e.g. the broad absorption and emission bands, long storage lifetime, low defect density, no excited state absorption or upconversion loss, and wide range of tunability, etc. [16–19]. Additionally, the similarity in diameter between Y and Yb ions allows a heavy doping of the latter into YAG matrix with low lattice mismatch, thus minimizing the distortion on fluorescence properties [20]. In addition, thin heavily doped Yb:YAG ceramic could serve as microchip laser material due to its excellent thermal property.

However, the quasi-four-level system of Yb:YAG limits the laser output by the thermal population of terminated lasing levels at 612 cm^{-1} of $^2F_{7/2}$ ground state, and it contains about 5% of $^2F_{7/2}$ population at room temperature [21]. Moreover, the fluorescence properties, e.g. the emission cross-section and fluorescence lifetime, can be strongly influenced by the doping concentration, as well as temperature [22,23]. In 2002, Yang et.al. pointed out the concentration quenching effect of Yb:YAG crystal for Yb concentration above 10 at.% due to unwanted impurities in raw materials[24]. In 2003, Dong et.al. reported that both emission cross-section and lifetime are greater at lower temperature than those at room temperature for Cr, Yb codoped single crystal [25]. Later, Qiu, Yang and Dong et.al. reported the dependence of optical properties on doping concentration for Yb:YAG single crystal [26,27]. In 2009, Dong reported that the fluorescence lifetime began to decrease when Yb concentration was beyond 15 at.%, and it decreased to 15% when Yb concentration reached to 25 at.%. It was attributed to both radiative trapping and concentration quenching effect [28].

This paper reports the dependence of the optical, fluorescence and thermal properties of Yb:YAG transparent ceramics on both temperature and dopant concentration. Efficient laser oscillation is achieved on 5 at.% and 10 at.% Yb:YAG ceramics by using 940 nm pumping source.

2. Experimental

2.1. Sample preparation

Commercial high-purity powders of α-Al_2O_3 (99.99%, Sumitomo Chemical Co. Ltd, Japan), Y_2O_3 (99.99%, Alfa Aesar, United States), Yb_2O_3 (99.99%, Alfa Aesar, United States) were used as starting materials, while 0.5 wt.% tetraetheoxysilane (TEOS,

* Corresponding author at: Key Lab of Optoelectronic Materials Chemistry and Physics, Fujian Institute of Research on the Structure of Matter, Chinese Academy of Sciences, Fuzhou 350002, China. Tel.: +86 010 62513093.
E-mail address: caoyongge@fjirsm.ac.cn (Y. Cao).

0925-8388/$ - see front matter © 2014 Elsevier B.V. All rights reserved.
http://dx.doi.org/10.1016/j.jallcom.2013.12.194

99.999+%, Alfa Aesar, United States) and 0.2 wt.% Oletic Acid (99%, Alfa Aesar, United States) were adopted as sintering aid and dispersant agent, respectively. The starting materials were weighted in accordance with the chemical composition of $(Yb_xY_{1-x})_3Al_5O_{12}$ (x = 0, 0.05, 0.10, 0.15, 0.20) and then homogeneously mixed in ethanol for 20 h in a planetary-milling machine. The weight ratio of powders and solvent is 1:1. The obtained slurry was dried in the oven at 65 °C for 24 h, then ground and sieved through 200-mesh screen. The powders were uniaxially pressed into Φ15 mm disks with thickness of about 2 mm and then calcinated at 700 °C for about 10 h in air before cold isostatic pressing under 200 MPa. The as-obtained Yb:YAG green bodies were sintered at 1720 °C for 10 h under vacuum condition of 5×10^{-7} torr, and then annealed at 1450 °C for 10 h in oxygen atmosphere.

2.2. Sample characterization

The phase identification was carried out by X-ray diffraction (XRD), and the surface morphology was characterized by means of scanning electron microscopy (JSM-6700F, JEOL). The optical transmittance was measured by UV/Vis/NIR spectrophotometer (Lambda-900, PekinElmer). The fluorescence spectra, as well as decay curves, were recorded using spectrophotometer (Edinburgh, FLS920) by taking a microsecond flash lamp (Edingburgh, μF900) as the exciting source. The signals were detected with an NIR PMT(Hamamatsu, R5509). The thermal diffusivity was measured by Laser Flash Apparatus (LFA457, Netzsch).

3. Results and discussion

3.1. Morphology and phase characterization

Fig. 1 shows the photos of Yb:YAG ceramics with Yb concentration ranging from 0 to 20 at.%. The green color of pre-annealing samples tends to be dark with increasing Yb content. We attributed this phenomenon to the emergence of color centers during vacuum sintering process [24,29,30]. However, the color has faded, and the samples become colorless and transparent after high temperature annealing treatment in oxygen atmosphere. SEM image of surface morphology of YAG ceramic is shown in Fig. 2 in which the clear grain boundary is observed without any pores or other second phase. All of the grains are tightly bonded with each other, of which the average size is about 10 μm. When a light beam transmits through the samples, they exhibit excellent transparency, which could be ascribed to the grain boundaries without any pores inside. In transparent ceramics, when the grain size is much lower than the light wavelength, the scattering can be totally ignored. Fig. 3 illustrates the XRD patterns of 5 at.%, 10 at.%, 15 at.% and 20 at.% Yb:YAG ceramics. It indicates that each graph matches well with YAG crystal phase, and no second phase peak is observed. With the rise of Yb doping concentration, some peaks show weak shifts, which, nonetheless, could be negligible and have no influence on YAG phase identification.

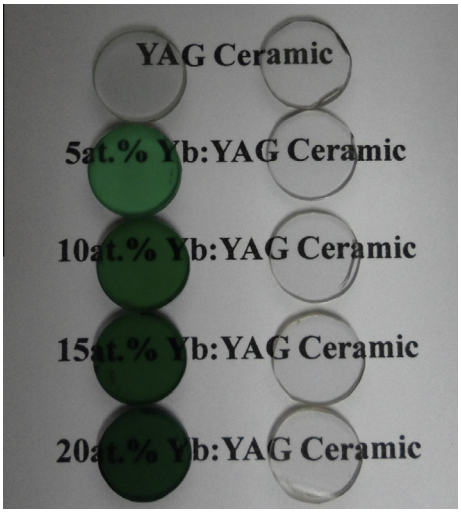

Fig. 1. Photos of YAG transparent ceramics doped with 0, 5 at.%, 10 at.% 15 at.% and 20 at.% Yb concentration (left denotes pre-annealed samples and right denotes post-annealed samples).

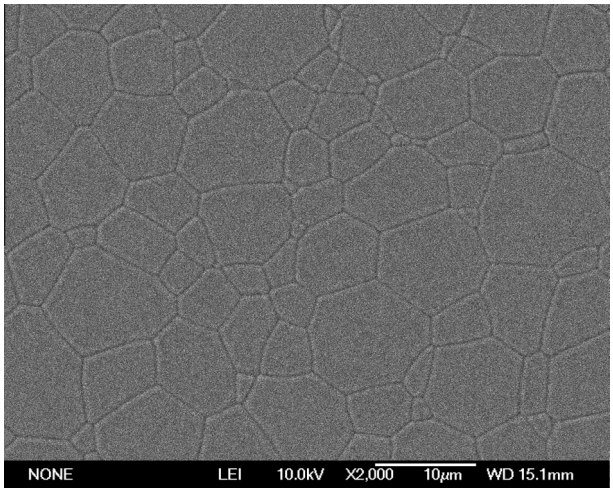

Fig. 2. Surface morphology of YAG ceramics.

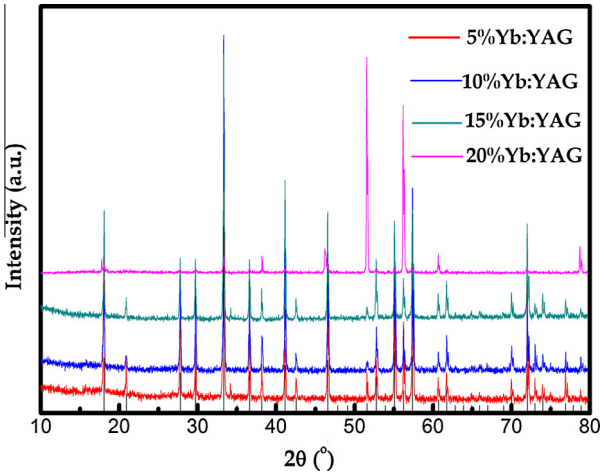

Fig. 3. XRD patterns for Yb:YAG ceramics with various doping concentration.

3.2. Optical and fluorescence analysis

The optical transmittance spectra were measured at room temperature ranging from 190 nm to 1100 nm for each sample, as shown in Fig. 4. The pure YAG ceramic has an absorption edge at about 190 nm, which red-shift to about 230 nm for Yb:YAG ceramics. The inlet figure shows this gradual red-shift with the rise of Yb concentration. According to the energy band theory, the pure YAG crystal has a stable crystal field and constant band-gap. However, the Yb doping into YAG matrix disturbs the crystal field, and induces impurity energy levels into the forbidden band. It finally results in red shift of the absorption edge. Additionally, optical transmittances are beyond 80% for all samples, with three strong absorption peaks around 915 nm, 940 nm, and 970 nm. Fig. 5 shows the absorption spectra, and absorption coefficient is observed to rise with increasing doping concentration. They are measured to be 6 cm^{-1},11 cm^{-1},16 cm^{-1} and 22 cm^{-1} for 5 at.%, 10 at.%, 15 at.%, and 20 at.% Yb:YAG ceramics respectively.

Fig. 6(a) illustrates fluorescence spectra of Yb:YAG ceramics with various doping concentrations in room temperature, ranging from 950 nm to 1300 nm. The strongest emission peaks locate at

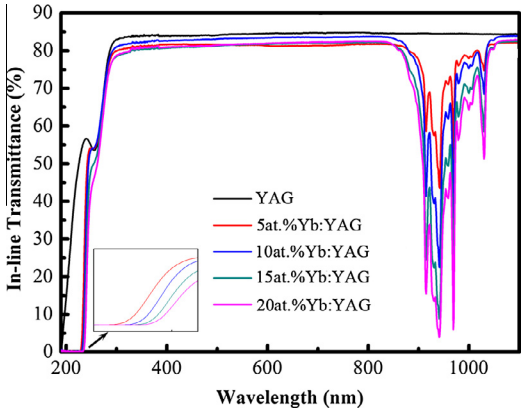

Fig. 4. Optical transmittance spectra for YAG ceramics with Yb doping concentration of 0, 5 at.%, 10 at.%, 15 at.% and 20 at.% (inlet figure shows the variation of absorption edge with Yb ions concentration).

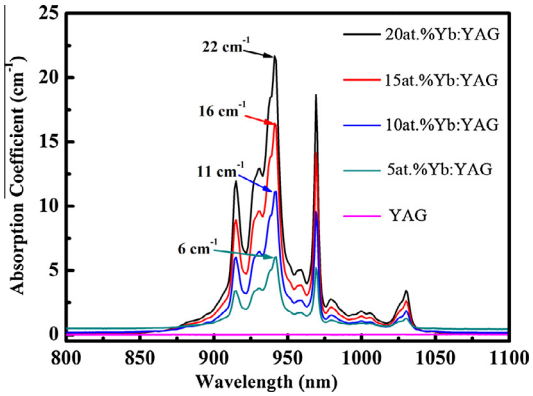

Fig. 5. Absorption spectra for YAG ceramics with Yb doping concentration of 0, 5 at.%, 10 at.%, 15 at.% and 20 at.%.

1030 nm for all samples, and the intensity begins to decrease when Yb concentration is beyond 10 at.%. However, the intensity of another emission peak located at about 1050 nm increases with the rise of Yb content, as shown in inset figure. As a result, the ratio of peak intensity at 1030 nm to that at 1050 nm varies among samples, and the higher value means easier oscillation at 1030 nm for laser experiment. It can thus be predicted that samples with 5 at.% and 10 at.%Yb are preferred to generate 1030 nm laser. Actually, both emission peaks above can be attributed to the transition from $^2F_{5/2}$ to $^2F_{7/2}$ manifolds for Yb^{3+}ions [21,31–36]. Fluorescence lifetime spectra of all samples are shown in Fig. 6(b). The lifetime was found to increase with increasing Yb concentration, and 1.92 ms of lifetime was obtained for 20 at.% Yb:YAG ceramic. Such long lifetime is mainly attributed to the self-absorption effect, which is unavoidable at high doping concentration. Sumida et.al. mentioned that this effect could be depressed using thin sample in the experiment [37], and this work is now being carried on.

3.3. Influence of temperature on fluorescence and thermal properties

It is of significant importance to study the dependence of fluorescence and thermal properties on temperature. As shown in Fig. 7, the emission peak intensity at about 1030 nm is very sharp at 100 K. However, it is depressed with broadening FWHM when the temperature gradually rises. At room temperature, the intensity is only half of that at 100 K, and the FWHM increases from 4 nm to nearly 10 nm. Additionally, a weak peak located at 1024 nm gradually disappears with increasing temperature. This

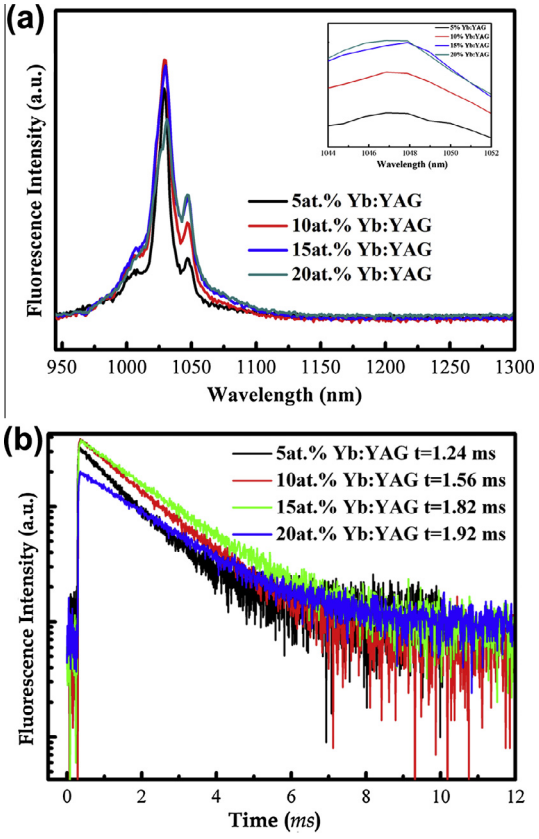

Fig. 6. Fluorescence spectra (a) and lifetime decay curves (b) for YAG ceramics with Yb doping concentration of 5 at.%, 10 at.%, 15 at.% and 20 at.% at room temperature (inlet figure shows the fluorescence spectra ranging from 1044 nm to 1052 nm).

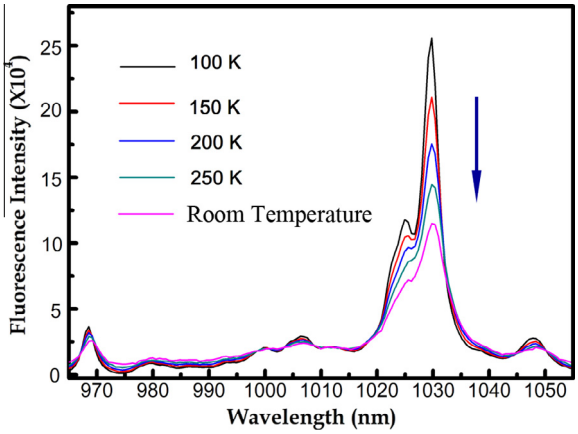

Fig. 7. Fluorescence spectra for 5 at.% Yb:YAG ceramic at various temperatures.

phenomenon indicates that peak at 1030 nm is preferred at room temperature. Except for the two peaks mentioned above, a weak peak at 1049 nm could also be found, as shown in Fig. 7. The ratio of intensity at 1030 nm to that at 1050 nm is clearly different, and it tends to rise with decreasing temperature. This contributes to the explanation of good laser output at about 1030 nm for Yb:YAG ceramics when temperature is set low enough.

The dependence of thermal diffusivity (α) on temperature, as well as on doping concentration, was shown in Fig. 8(a). It was found that temperature has apparent influence on thermal diffusivity. Each ceramic performs the decline trend of thermal diffusivity with increasing temperature. For YAG ceramic, while

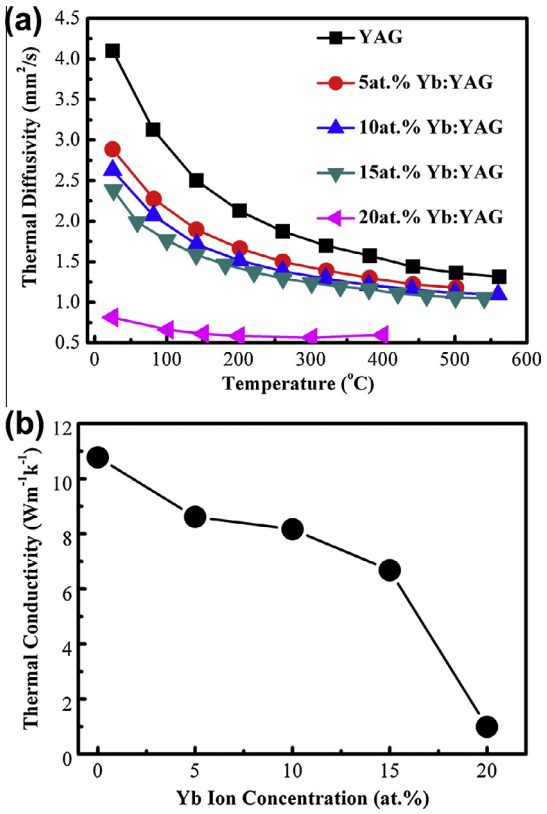

Fig. 8. Curves of the thermal diffusivity *vs* temperature for YAG ceramics with various Yb doping concentration (a) and the curve of thermal conductivity *vs* Yb concentration at room temperature (b).

temperature increases from room temperature to about 560 °C, the thermal diffusivity decreases by as much as 67%. However, the effect of temperature on thermal diffusivity is found to be gradually weakened with rise of doping concentration. For samples with Yb doping content of 0, 5 at.%, 10 at.%, 15 at.% and 20 at.%, when the temperature changes from the room temperature to about 400 °C, the corresponding thermal diffusivity decreases by 62%, 56%, 55%, 52%, and 28%.

The relationship between the thermal diffusivity (α) and thermal conductivity (D) is expressed by:

$$D = \alpha \rho C_P \quad (1)$$

where ρ is the density of Yb:YAG ceramic, and C_P is the specific heat. The room temperature thermal conductivity was measured, as shown in Fig. 8(b). We could find that YAG ceramic has a thermal conductivity of about 10.7 W m^{-1} K^{-1}, and it is comparable to the theoretical value of YAG single crystal [38]. However, while the doping concentration of Yb ions increases from 5 at.% to 20 at.%, the thermal conductivity decreases by as much as 88%, from 8.6 W m^{-1} K^{-1} to 0.99 W m^{-1} K^{-1}. From Fig. 8(a), we could also predict that with the increase of temperature, thermal conductivity decreases. In Yb:YAG ceramic matrix, the heat conduction is mainly due to lattice vibration (phonons transport). Yb ions doping into YAG matrix induces some extent of structural distortion, and generation of point defects. These defects can reduce the phonon mean free path, and therefore depress the thermal conductivity. Similarly, the increase of temperature causes the lattice vibration of a higher degree and larger point defects density. The deterioration of thermal properties of Yb:YAG ceramic is tightly related with thermooptic aberrations, lensing and birefringence. Therefore, an efficient cooling arrangement is required during laser experiment to obtain high beam quality and stable laser output.

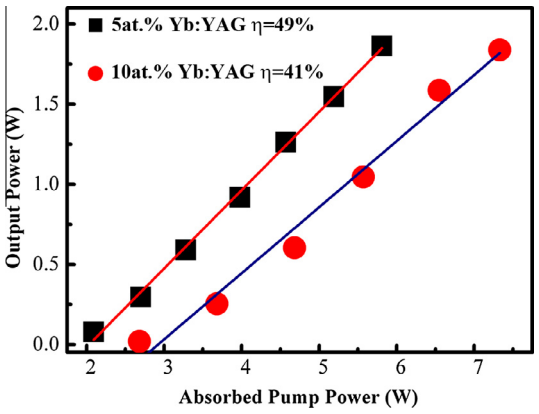

Fig. 9. CW laser output power as a function of absorbed pump power for 5 at.% Yb:YAG and 10 at.% Yb:YAG ceramics.

3.4. Laser performance of Yb:YAG ceramics

The measurement of laser performance was carried out on annealed Yb:YAG ceramics with doping concentration of 5 at.% and 10 at.%, as shown in Fig. 9. A fiber-coupled 940 nm diode laser was used as the pumping source, and we adopted plano–plano resonator. The input mirror has a transmission of 95% at 940 nm and 99.8% at 1030 nm while the output coupler has a fixed transmission of 5%. The temperature was controlled at about 20 °C by the circulating water system. Fig. 9 shows that slope efficiency of 49% has been obtained for 5 at.% Yb:YAG ceramic, and the threshold absorbed pump power is 2.1 W. However, when Yb doping concentration is changed to 10 at.%, slope efficiency decreases to 41%, and the threshold absorbed pump power increases to 2.6 W. Therefore, 5 at.% Yb:YAG ceramic performs better laser output than 10 at.%Yb:YAG ceramic.

4. Conclusions

YAG transparent ceramics with various Yb doping concentration were successfully fabricated using vacuum sintering technology. The influence of concentration, as well as temperature, on their optical, fluorescence, and thermal properties was systematically investigated. The results indicate that the increase of Yb doping concentration leads to the red-shift of absorption edge and rise of Yb^{3+} absorption coefficient as well. The fluorescence lifetime could also become longer with increasing Yb concentration. However, the optimum emission at 1030 nm occurred in 5 at.% and 10 at.% Yb:YAG ceramics. With the rise of temperature, the emission intensity at 1030 nm falls, and the thermal property deteriorates for 5 at.% Yb:YAG ceramics. At room temperature, the thermal conductivity of YAG ceramic attains to 10.7 Wm^{-1} K^{-1}. The heavier Yb doping results in the lower thermal conductivity of Yb:YAG ceramics. Finally, our laser experiment indicates that 5 at% Yb:YAG ceramics demonstrate better laser output than 10 at.%Yb:YAG ceramics do.

Acknowledgements

This work was financially supported by the program of National Natural Science Foundation of China (No. 51272282), the program of National Natural Science Foundation of China (No. 51302311), the program of Beijing Municipal Commission of Science and Technology (No. 008004-3581300100), and the program of Beijing Municipal Commission of Education (No. 2011010329).

References

[1] A. Ikesue, T. Kinoshita, K. Kamata, K. Yoshida, J. Am. Ceram. Soc. 78 (1995) 1034–1040.
[2] Y.W. Zou, Z.Y. Wei, Q. Wang, M.J. Zhan, D.H. Li, Z.G. Zhang, J. Zhang, D.Y. Tang, Opt. Mater. 35 (2013) 804–806.
[3] S.Y. Zhang, X. Wang, W.J. Kong, Q.L. Yang, J.Q. Xu, B.X. Jiang, Y.B. Pan, Opt. Commun. 286 (2013) 288–290.
[4] E. Cavalli, L. Esposito, J. Hostasa, M. Pedroni, J. Eur. Ceram. Soc. 33 (2013) 1425–1434.
[5] X.W. Ba, J. Li, Y.B. Pan, Y.P. Zeng, H.M. Kou, W.B. Liu, J. Liu, L.X. Wu, J.K. Guo, J. Alloys Comp. 577 (2013) 228–231.
[6] M. Prakasam, O. Viraphong, D. Michau, A. Largetear, Ceram. Int. 40 (2014) 1859–1864.
[7] Y. Jia, J.R. Vazquez de Aldana, S. Akhmadaliev, S.Q. Zhou, F. Chen, Opt. Mater. 36 (2013) 228–231.
[8] A. Agnesi, L. Carra, F. Pirzio, G. Reali, S. Veronesi, J. Tharayil Thomas, M. Tonelli, J. Li, Y. Pan, J. Guo, Opt. Commun. 315 (2014) 208–212.
[9] J. Dong, A. Shirakawa, K. Ueda, Appl. Phys. Lett. 89 (2006) 0911141–0911143.
[10] P.Z. Yang, P.Z. Deng, Z.W. Yin, Y.L. Tian, J. Cryst. Growth 216 (2000) 348–351.
[11] F. Tang, Y.G. Cao, J.Q. Huang, W. Guo, H.G. Liu, W.C. Wang, Q.F. Huang, J.T. Li, Laser Phys. Lett. 9 (2012) 103–106.
[12] C. Gheorghe, A. Lupei, F.M. Voicu, C. Tiseanu, J. Alloys Comp. 588 (2014) 388–393.
[13] T. Kallel, M.A. Hassairi, M. Dammak, A. Lyberis, P. Gredin, M. Mortier, J. Alloys Comp. 584 (2014) 261–268.
[14] D.C. Brown, C.D. McMillen, C. Moore, J.W. Kolis, V. Envid, J. Lumin. 148 (2014) 26–32.
[15] Y.Q. Shen, X.Q. Feng, Y. Shi, A. Vedda, F. Moretti, C. hu, S.P. Liu, Y.B. Pan, H.M. Kou, L.X. Wu, Ceram. Int. 40 (2014) 3715–3719.
[16] F. Tang, Y.G. Cao, J.Q. Huang, H.G. Liu, W. Guo, W.C. Wang, J. Am. Ceram. Soc. 95 (2012) 56–59.
[17] F. Tang, Y.G. Cao, J.Q. Huang, W. Guo, H.G. Liu, Q.F. Huang, W.C. Wang, J. Eur. Ceram. Soc. 32 (2012) 3995–4002.
[18] H. Chu, S.Z. Zhao, K.J. Yang, Y.F. Li, D.C. Li, G.Q. Li, J. Zhao, W.C. Qiao, X.D. Xu, J.Q. Di, L.H. Zheng, J. Xu, Opt. Laser Tech. 56 (2014) 398–403.
[19] L. Esposito, A. Piancastelli, Y. Bykov, S. Egorov, A. Eremeev, Opt. Mater. 35 (2013) 761–765.
[20] J. Hostasa, L. Esposito, D. Alderighi, A. Pirri, Opt. Mater. 35 (2013) 798–803.
[21] J. Dong, A. Shirakawa, K. Ueda, A.A. Kaminskii, Appl. Phys. B 89 (2007) 367–376.
[22] W. Strek, L. Marciniak, P. Gluchowski, D. Hreniak, Opt. Mater. 35 (2013) 2013–2017.
[23] Y. Fujimoto, T. Yanagida, S. Wakahara, H. Yagi, T. Yanagidani, S. Kurosawa, A. Yoshikawa, Opt. Mater. 35 (2013) 778–781.
[24] P.Z. Yang, P.Z. Deng, Z.W. Yin, J. Lumin. 97 (2002) 51–54.
[25] J. Dong, P.Z. Deng, J. Phys. Chem. Solid 64 (2003) 1163–1171.
[26] H. Qiu, P. Yang, J. Dong, P. Deng, J. Xu, W. Chen, Mater. Lett. 55 (2002) 1–7.
[27] J. Dong, A. Shirakawa, K. Ueda, A.A. Kaminskii, Appl. Phys. B 89 (2007) 359–365.
[28] J. Dong, K. Ueda, H. Yagi, A.A. Kaminskii, Z. Cai, Laser Phys. Lett. 6 (2009) 282–289.
[29] X.D. Xu, Z.W. Zhao, P.X. Song, G.Q. Zhou, J. Xu, P.Z. Deng, J. Opt. Soc. Am. B 21 (2004) 543–547.
[30] F. Tang, Y.G. Cao, W. Guo, Y.J. Chen, J.Q. Huang, Z.H. Deng, Z.G. Liu, Z. Huang, Opt. Mater. 33 (2011) 1278–1282.
[31] F. Tang, J.Q. Huang, W. Guo, W.C. Wang, B.J. Fei, Y.G. Cao, Opt. Mater. 34 (2012) 757–760.
[32] J. Dong, M. Bass, Y.L. Mao, P.Z. Deng, F.X. Gan, J. Opt. Soc. Am. B 20 (2003) 1975–1979.
[33] J. Saikawa, Y. Sato, T. Taira, A. Ikesue, Appl. Phys. Lett. 85 (2004) 1898–1900.
[34] M. Ostermeyer, A. Straesser, Opt. Commun. 274 (2007) 422–428.
[35] S.Z. Zhao, A. Rapaport, J. Dong, B. Chen, P.Z. Deng, M. Bass, Opt. Mater. 27 (2005) 1329–1332.
[36] S. Hinojosa, O. Barbosa-Garcia, M.A. Meneses-Nava, J.L. Maldonado, E. de la Rosa-Cruz, G. Ramos-Ortiz, Opt. Mater. 27 (2005) 1839–1844.
[37] D.S. Sumida, T.Y. Fan, Opt. Lett. 19 (1994) 1343–1345.
[38] Y. Sato, T. Taira,in: Frontiers in Optics Rochester (Conference), New York, 2006.